Polymer Bulletin
https://doi.org/10.1007/s00289-020-03299-w

ORIGINAL PAPER

Mechanical behavior of ABS plastic-matrix nanocomposites with three different carbon-based nanofillers

Minju Oh[1] · Whi Dong Kim[1] · Mao Zhang[1] · Taehyeong Kim[1] · Dayoung Yoo[1] · Soo Hyung Kim[1,2] · Dongyun Lee[1,2]

Received: 2 March 2020 / Revised: 18 May 2020 / Accepted: 1 July 2020

Abstract

Acrylonitrile butadiene styrene (ABS) polymer nanocomposite thin films with carbon-based nanofillers (CBNs: fullerene, carbon nanotubes, and graphene) were fabricated in a wet reversal process followed by hot pressing. To understand the effect of CBNs on the fabricated nanocomposites, tensile tests and nanoindentation tests were performed. The tensile strength of the fullerene composite was about 30 MPa based on the specimen containing 1 wt% of CBNs, which was measured to be up to 35% higher than the other two composites. In the nanoindentation test, the elastic modulus and hardness value decreased as the amount of CBNs increased. This is considered to be because the nanoindentation test reflects more mechanical behavior of the local part of the composite than the tensile test. In the tensile and nanoindentation tests, all of the nanofillers exhibited the mechanical properties of ABS polymers, among which the ABS composites with fullerene exhibited the best properties. It is concluded that nanofillers should be added appropriately, and in the case of polymers, nanofillers, which may be located between polymer chains such as fullerene, may be more efficient.

Electronic supplementary material The online version of this article (https://doi.org/10.1007/s00289-020-03299-w) contains supplementary material, which is available to authorized users.

✉ Dongyun Lee
dlee@pusan.ac.kr

[1] Department of Nano Fusion Technology, Pusan National University, 2 Busandaehak-ro 63beon-gil, Geumjung-gu, Busan 46241, Republic of Korea

[2] Department of Nanoenergy Engineering, Pusan National University, 2 Busandaehak-ro 63beon-gil, Geumjung-gu, Busan 46241, Republic of Korea

Published online: 06 July 2020

Graphic abstract

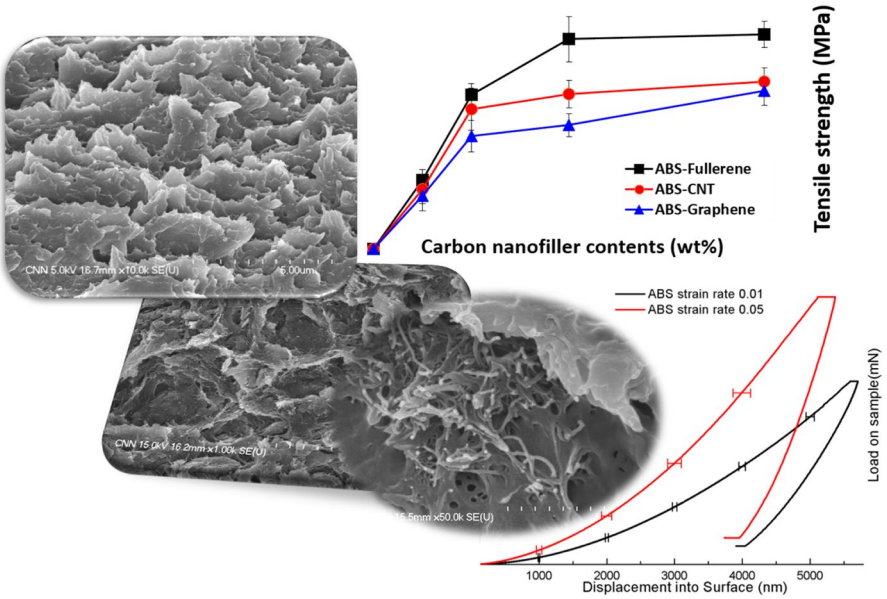

Keywords ABS polymer · Carbon-based nanofillers · Nanocomposite · Tensile test · Nanoindentation test

Introduction

A composite material is obtained by artificially combining two or more distinct materials. This approach allows to improve material properties and design materials with novel properties. In particular, polymer composites are expected to replace existing metal materials, owing to their better mechanical properties [1]. Lightweight, owing to light polymer composites, has become a social issue in recent years, in the trends for energy efficiency and scarce resource reduction. Light materials appear to significantly contribute to solving the energy problem. In general, nanosized materials are advantageous for use as a reinforcing agent of composite materials because of their high specific surface area and low internal defects, which are excellent in mechanical properties [2]. Nanomaterials have their strengths, particularly as fillers in polymer-based composites that have weaknesses in mechanical strength. As mentioned above, the nanosized material has a large specific surface area, which has the advantage of increasing the interfacial bond with the polymer chains [3, 4]. This molecular-level interaction plays an important role in dramatically improving the mechanical properties of hybrid polymer–nanofiller composites. Dispersion of fillers used as reinforcing agents in polymer-based composites is very important, especially for nanofillers that have a high specific surface area and are

highly reactive and agglomerate [5, 6]. Therefore, the size or dimension of nanofillers used in polymer-based composites is very important. Many research groups around the world have investigated the effect of nanofillers with 0-dimensional (0D) or 1-dimensional (1D) dimensions on the mechanical behavior of polymer-based composites. For example, the addition of small amounts of metal nanoparticles (MNP, 0D) and carbon nanotubes (CNT, 1D) has been reported to significantly improve the mechanical properties of polymer-based composites with varying degrees [7–20]. Recently, carbon nanotubes, graphene, and carbon nanomaterials with excellent mechanical properties have been considered as next-generation filler materials.

In the present study, acrylonitrile butadiene styrene (ABS) was chosen as an example polymer matrix, owing to its superior properties. ABS is a triblock copolymer, belonging to the chemical family of styrene terpolymers, which are characterized by good strength and toughness [21]. ABS is easy to handle (e.g., in machining, painting, and gluing), and it has many other valuable characteristics, for example, strong impact, and scratch and heat resistance [22–25].

Three different types of carbon-based nanofillers were considered in 0D (fullerene), 1D (carbon nanotubes), and two-dimensional (2D) materials (graphene), and nanocomposites with ABS were fabricated. One could expect the nanofillers to differentially affect the mechanical properties of composite carbon nanomaterials, owing to their different shapes, structures, and properties. It is plausible to assume that a 0D material added to a polymer matrix will only interact at several points along a particular polymer chain, whereas CNTs and graphene added to a polymer matrix will interact over the entire length of the polymer chain. The mechanical properties were based on a tensile test and a nanoindentation system. Each method is suitable for measuring the overall and local properties of the specimen, so it is considered to be effective in identifying the properties of the nanopillar composites.

Experimental details

ABS plastic (211.31 g/mol, Sigma Aldrich, St. Louis, USA) for the nanocomposite matrix was dissolved in dimethylformamide (DMF, Sigma Aldrich, St. Louis, USA) and stirred for 3 h to obtain a 5 wt% concentration solvent. Fullerene, carbon nanotubes, and multi-layered graphene were added as fillers (0.25 wt%, 0.5 wt%, 1 wt%, 2 wt% out of ABS/CBNs composites' weight) to the ABS plastic matrix. Figure S1 shows transmission electron microscopy (TEM) (Jeol, JEM-2100F operated at 200 kV) images of the nanofillers used in this study. The specific surface areas of the nanofillers were also measured using a Brunauer–Emmett–Teller (BET) surface area and porosimetry analyzer (ASAP2000, micromeritics®), to understand how the nanofillers affect the mechanical properties of the polymer matrix (Table 1). The solutions were sonicated for 3 h, to reduce the agglomeration of the nanofillers before the fabrication of the composites. For uniform dispersion of the nanofillers in the ABS polymer matrix, we used the phase-shift method (wet phase inversion process), which allows to rapidly precipitate a solution in a polymer matrix, increasing the

Table 1 Specific surface area of carbon-based nanoreinforcements: fullerene, CNT, and graphite

	Fullerene	CNTs	Graphene
Dimension	$D_F = 0.7$ nm	$D_c = 25$ nm	$t_G = 40$ nm
Theoretical formula of specific surface area	$6/D_F$	$4/D_c$	$2/(t_G \times 7)$
Specific surface area (m^2/g)	8.57×10^9	1.60×10^8	0.07×10^8

homogeneity of the two mixed substances. Schematic of the process is shown in Fig. S2, and a detailed description of the fabrication process was given previously [26, 27]. As described in Ref. 15, we fabricated such complexes with uniformly dispersed nanofiller-reinforced polymer composites, using the wet phase inversion process.

Three different types of carbon-based nanofillers (CBNs) were dispersed in the ABS solution at various concentrations, i.e., 0.25 wt%, 0.5 wt%, 1 wt%, and 2 wt%, by 3-h-long sonication (170 W, 40 kHz). The ABS/CBN solution was mixed with filtered water to initiate the wet phase inversion process, in which a homogeneous mixture of ABS/CBNs was rapidly precipitated because of the solubility difference [9]. After the precipitated ABS/CBN composites were dried at 80 °C for 5 h, they were transformed into thin films (film diameter: 58 mm; film thickness: 300 μm) using a hot press system (SSAUL BESTECH, Inc., Model No. Mounting Press I) at 200 °C and 150 bar, for 8 min.

The mechanical properties of the fabricated nanocomposite films were investigated using a tensile test system (LRXPlus, Lloyd Instruments, UK) and a nanoindentation system (Nanoindenter ® G200 system, KLA Co., USA). The specimens for the tensile test (gauge section: 40.0 mm × 6.0 mm; thickness: 300 μm) were cut from the fabricated composite films. The tensile tests (testing guidelines ASTM D882 [28]) were conducted in air, using a 1-kN load cell at a crosshead speed of 10 mm/min. The results presented here are the average values obtained by analyzing at least seven specimens. The fracture morphologies of the nanocomposites used in this study were characterized using scanning electron microscopy (SEM, Hitachi, S-4200) operated at 15–20 kV. For the nanoindentation experiments, the films were glued onto an aluminum holder. The experiments were conducted using a Nanoindenter XP™, with the strain rate maintained under ~ 20% of the composite film thickness. At a given force level, the data were averaged over at least 20 indents, with the data scatter indicated by the standard deviation of displacement. A three-sided pyramid (Berkovich) diamond tip was used in the present study. The ABS polymer and the ABS/CBN composites were tested at two different strain rates, 0.01 s^{-1} and 0.05 s^{-1}. A constant indentation strain $\frac{\left(\frac{dh}{dt}\right)}{h}$ is obtained by a constant $\frac{\left(\frac{dP}{dt}\right)}{P}$ (h = displacement, t = time, P = load) test [29]. This allowed us to evaluate the hardness of the materials, independent of the indentation depth [30]. Unloading was tested using the same strain control as in the loading tests. The mechanical behavior and properties of the specimens, including their viscoelastic behavior and elastic moduli E, were interpreted from the unloading slopes of the corresponding load–displacement (L–D) curves.

Results and discussion

The results of the measurements of the specific surface area are shown in Table 1. As can be seen from the results, for the three types of nanopillars the specific surface area decreased in the following order: fullerene > CNT > graphene. In general, a large specific surface area is expected to positively affect the mechanical properties of the corresponding composite material, because it increases the contact area with the matrix materials [31–34].

Figure 1 shows the tensile test results for the fabricated nanocomposites prepared by mixing different nanofillers and ABS polymer. The specimens that were used in this study were prepared by mixing 0.25 wt%, 0.5 wt%, 1.0 wt%, and 2.0 wt% of each nanofiller type in the weight ratio. As expected from the specific surface area results, the tensile strength was the highest for the ABS/fullerene nanocomposite, followed by the ABS/CNT and ABS/graphene composites. The tensile strength increased with increasing nanofiller content. The rate of increase was rapid for concentrations up to 0.5 wt% and thereafter remained almost constant. However, the addition of fullerene significantly increased the tensile strength, up to 1.0 wt%.

Besides, we performed the mechanical property measurement for the case of filler concentration > 2 wt%. However, the tensile strength and elongation of the ABS/CBNs composite thin films were unstable. That is, the data deviation is too large to be used. It appears that CBN is strongly agglomerated at a higher concentration (> 2 wt%) in the polymer matrix, resulting in cracking when tensile strength is applied to the specimen. So, in this study, the experiment was conducted by maintaining the content of CBNs at 2 wt% or less.

The SEM micrographs of the fracture surface of the ABS and ABS/fullerene nanocomposites are shown in Fig. 2. The ABS polymer exhibits the typical fracture surface of a polymeric material (Fig. 2a), with ductile fracture in the tensile

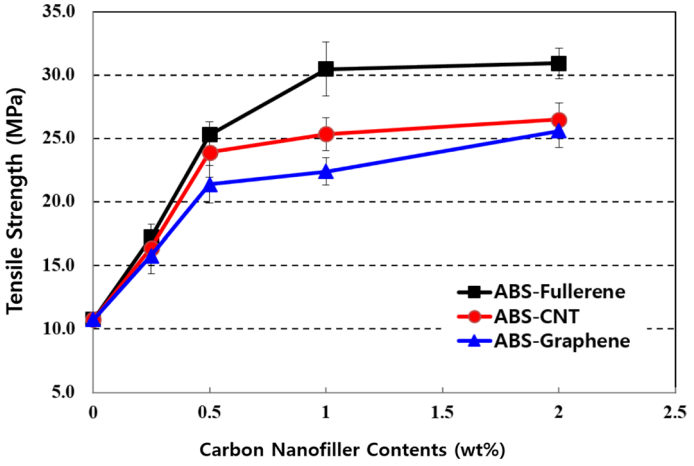

Fig. 1 Tensile strength of ABS/CBN nanocomposites. Fullerene-added nanocomposites exhibit the highest tensile strength gain, while graphene exhibits the lowest tensile strength gain

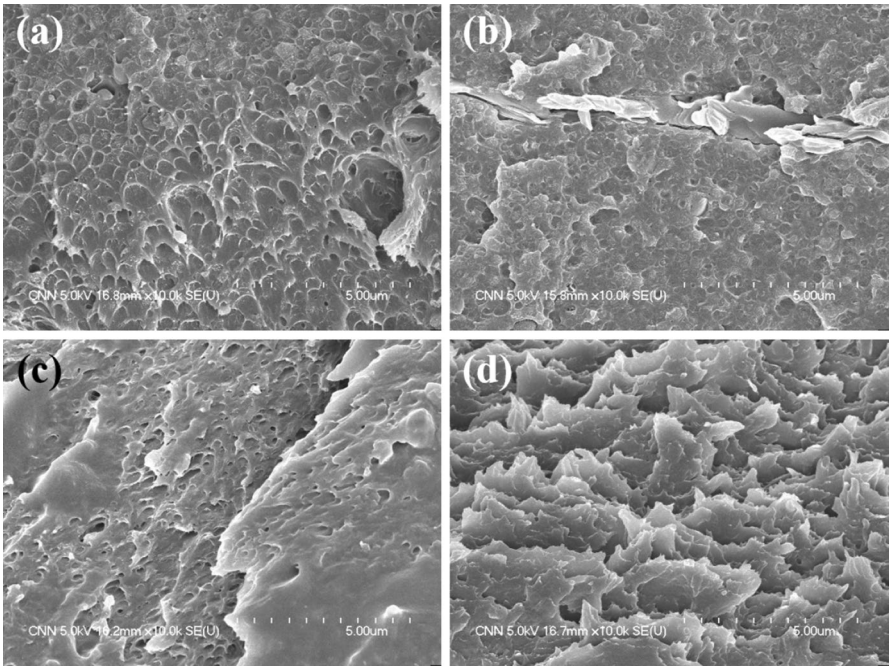

Fig. 2 SEM micrographs of fracture surfaces of the ABS polymer and ABS/fullerene nanocomposites: **a** bare ABS; **b** ABS/fullerene at 0.5 wt%; **c** ABS/fullerene at 1 wt%; **d** ABS/fullerene at 2 wt%

direction with small dimples with shear lips [35, 36]. As shown in Fig. 2b–d, with increasing the amount of fullerene, the amount of shear lips increased (in particular for 2.0 wt% fullerene specimens). Therefore, the addition of fullerene was observed to increase the tensile strength of the ABS polymer more than threefold. However, since the increase was not significant at and above 1.0 wt%, it is important to add an appropriate amount of nanofillers to the matrix.

The tensile fracture surfaces of the ABS/CNT and ABS/graphene nanocomposites are shown in Fig. 3. Figure 3a, b shows the fracture surfaces of the specimens with 0.5 wt% and 2.0 wt% CNTs added to the ABS matrix, respectively. Although the shear lips look similar to those shown in Fig. 2, the morphology appears to be the pull-out of the CNTs as shown in the insets of Fig. 3a, b. It is believed that the dispersion of CNTs is not perfect, and they are aggregated and pulled out by the tensile stress [37, 38]. In the case of 2.0 wt% CNTs, the agglomeration was more severe than in the case of 0.5 wt% CNTs, and the tensile strength no longer increased.

The fracture surfaces of the specimens with 0.5 wt% and 2.0 wt% of graphene added to the ABS matrix are shown in Fig. 3c, d, respectively. Unlike the results in previous figures, there are several fracture planes closer to the cleavage fracture than the shear lip (especially for 2.0 wt% graphene specimens, inset in Fig. 3d). Therefore, the tensile strength and the rate of increase are lower than those for the other two cases. In this fabrication process, there is a pressing step, which causes the unfolding of graphene and CNTs in the direction perpendicular to that

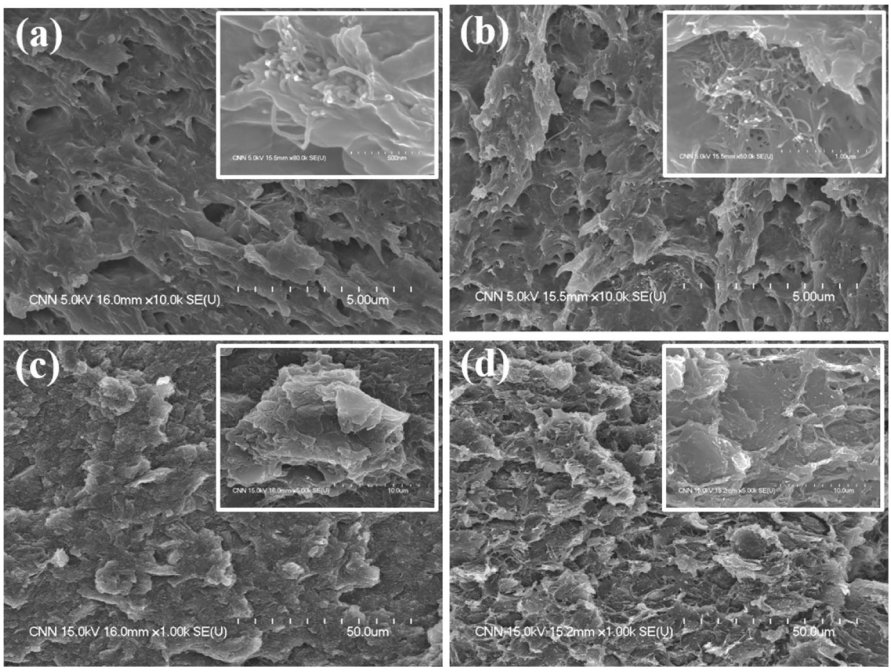

Fig. 3 SEM micrographs of fracture surfaces of the ABS polymer and ABS/CNT/graphene nanocomposites: **a** ABS/CNT at 0.5 wt%; **b** ABS/CNT at 2.0 wt%; **c** ABS/graphene at 0.5 wt%; **d** ABS/graphene at 2.0 wt%. **a**, **b**: pull-out and agglomeration of CNTs, potentially signaling a fracture point. **c**, **d**: graphene-added composite with cleavage fracture (see inset of **d**)

of the pressing direction, which probably increases the contact surface between the nanofillers and the ABS polymer matrix. It is also certain that the backbone of the ABS polymer is also elongated, and fullerene is dispersed throughout the backbone chain. Some micrographs that can more clearly show the fracture behavior of each CBNs are presented in Fig. S3 of supporting information.

Figure 4 shows the results of nanoindentation measurements for the ABS polymer and ABS/CBN nanocomposites. In the case of the nanocomposites, the samples with the 1.0 wt% filler were selected, because the tensile properties of the nanocomposites were saturated and changed most clearly following the addition of fillers (Fig. 5). Figure 4a shows the results of the nanoindentation experiment for the ABS polymer. As mentioned in the description of the test method, two different strain rates were adopted during the nanoindentation tests. The results show that the L–D curves are strongly affected by the strain rate. In general, strain rate sensitivity is a common phenomenon in polymeric materials [39, 40]. As shown in Fig. 4b–d, the fabricated filler-filled composites exhibited weaker strain rate sensitivity, especially following the addition of CNTs, with almost no strain rate effects. The plastic deformation and strain rate sensitivity mechanisms in polymers are basically owing to the interaction between the polymer backbones; they slid or entangle each other, yielding interesting mechanical behavior [41–43]. In this study, adding CNTs did not significantly affect strain sensitivity, suggesting

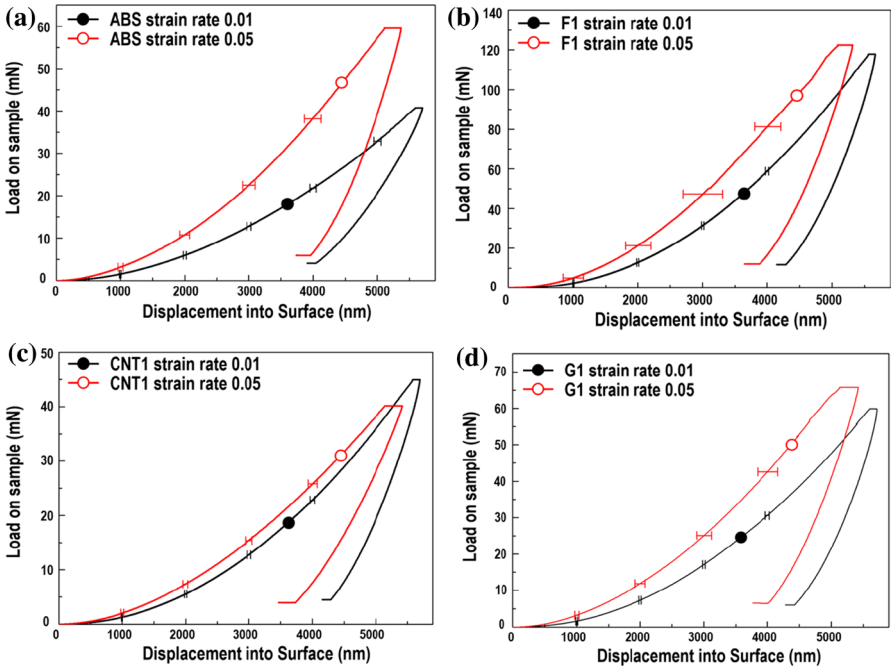

Fig. 4 Load–displacement curves of the ABS polymer and ABS/CBN nanocomposites: **a** ABS polymer; **b** ABS/fullerene at 1.0 wt%; **c** ABS/CNT at 1.0 wt%; **d** ABS/graphene at 1.0 wt%

that CNT nanofillers prevented the increase in friction caused by the sliding of the polymer backbone (chain).

Figure 5 shows the elastic modulus and hardness, measured at the strain rates of 0.01 and 0.05 s^{-1}, for composites with 0.5, 1.0, and 2.0 wt% of CNTs, fullerene, and graphene, respectively, in the ABS polymer. As shown in Fig. 4, strain sensitivity depends on the nanofiller type. The modulus and hardness at 0.05 s^{-1} are higher than those at 0.01 s^{-1}. As mentioned previously, this is a common observation for polymers. The fullerene-added ABS polymer composite exhibited the best mechanical properties among the three studied nanocomposites, which was the same as for the tensile tests. Yet, for filler content above 1 wt%, the modulus and hardness were dramatically reduced. CNT- and graphene-added nanocomposites also exhibited different mechanical behaviors compared with the tensile tests: (1) Modulus and hardness of CNT-added nanocomposites were lower than those of graphene-added samples; (2) there was no discernible effect of CNTs on the ABS polymer because most of the mechanical properties of CNT-added nanocomposites were worse than those of the pure ABS polymer; (3) graphene-added nanocomposites degraded sharply with increasing the filler content.

The tensile test reveals more universal mechanical properties of bulk specimens than the nanoindentation test, because nanoindentation experiments are more suitable for understanding small-volume specimens [44, 45]. The nanoindentation test explains why the tensile strength did not increase for the nanofiller content at or

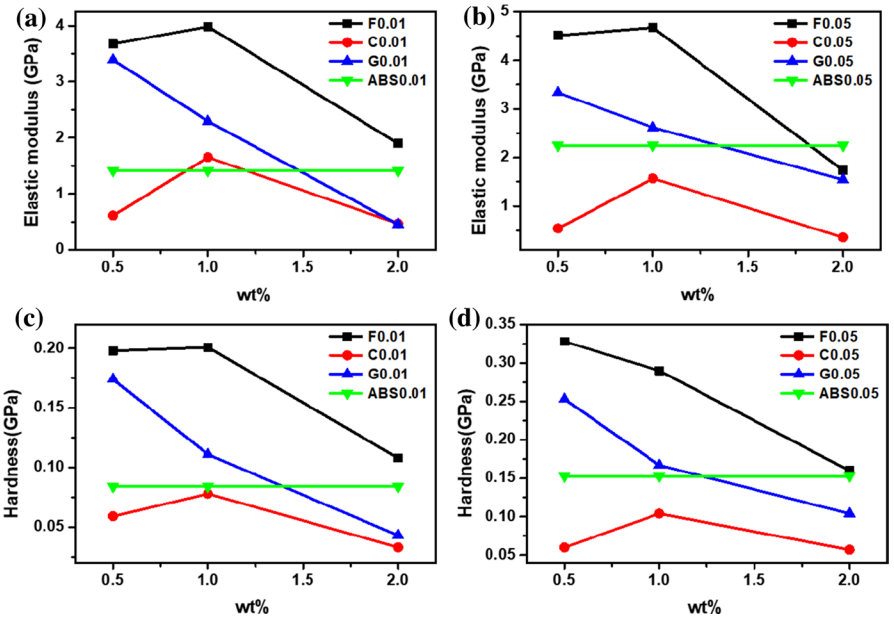

Fig. 5 Elastic modulus and hardness, measured in the nanoindentation experiments, for the strain rates of 0.01 s^{-1} and 0.05 s^{-1}: **a** elastic modulus for the 0.01 s^{-1} strain rate; **b** elastic modulus for the 0.05 s^{-1} strain rate; **c** hardness for the 0.01 s^{-1} strain rate; **d** hardness for the 0.05 s^{-1} strain rate

above 1 wt%. It is plausible that higher nanofiller content may act as a defect in the nanocomposite, owing to the nanofiller agglomeration, unless the nanofiller is well-dispersed. Optimizing the nanofiller content and controlling the interaction between polymer backbones clearly can help to manipulate the mechanical properties of polymer matrix nanocomposites. From this point of view, since fullerene could be readily accommodated between the polymer chains, it could improve the interactions between the chains (such as slippage disturbances).

Conclusion

In this study, we tried to understand how CBNs such as fullerene, carbon nanotubes, and graphene that were used in this study affect the mechanical properties of ABS polymer-based composite thin films. After the CBNs were mixed with the ABS polymer samples using the wet reversal process, thin films were prepared by hot pressing. To understand the effect of CBNs on the fabricated nanocomposites, tensile tests and nanoindentation tests were performed.

In the tensile and nanoindentation tests, all nanofillers enhanced the mechanical properties of the ABS polymer samples, among which the ABS composites with fullerene exhibited the best properties. The ABS/fullerene composite exhibited the highest tensile strength, which was about 33 MPa. The elastic modulus and hardness of the largest composite obtained through nanoindentation were about 4 GPa and

200 MPa, respectively. In the tensile test, the tensile strength tended to increase with increasing nanopillar content, but the increase saturated above a certain content. On the other hand, in the case of nanoindentation experiments, the mechanical properties of the fabricated nanocomposites deteriorated when the nanofiller content was 1 wt% or higher. In the case of graphene, the mechanical properties of the nanocomposite material decreased continuously with increasing the amount of added graphene. Tensile tests capture the mechanical properties of the entire tested specimen, while nanoindentation experiments reveal the tested specimen's local properties. The two tests are expected to complement each other. In conclusion, nanofillers should be added at an appropriate level, and in the case of polymers, nanofillers, which may be located between polymer chains such as fullerene, may be more efficient.

Acknowledgements This work was supported by the Financial Supporting Project of Long-term Dispatch of PNU's Tenure-track Faculty, 2018.

Compliance with ethical standards

Conflict of interest The authors declare that they have no conflict of interest.

References

1. Son DR, Raghu AV, Reddy KR, Jenong HM (2016) Compatibility of thermally reduced graphene with polyesters. J Macromol Sci B 55:1099–1110
2. Bonab SA, Moghaddas J, Rezaei M (2019) In-situ synthesis of silica aerogel/polyurethane inorganic–organic hybrid nanocomposite foams: characterization, cell microstructure and mechanical properties. Polymer 172:27–40
3. Reddy KR, Lee KP, Gopalan AI (2007) Self-assembly directed synthesis of poly(*ortho*-toluidine)-metal (gold and palladium) composite nanospheres. J Nanosci Nanotechnol 7:3117–3125
4. Reddy KR, Jeong HM, Lee YI, Raghu AV (2010) Synthesis of MWCNTs-core/thiophene polymer-sheath composite nanocables by a cationic surfactant-assisted chemical oxidative polymerization and their structural properties. J Polym Sci Polym Chem A 48:1477–1484
5. Han SJ, Lee HI, Jeong HM, Kim BK, Raghu AV, Reddy KR (2014) Graphene modified lipophilically by stearic acid and its composite with low density polyethylene. J Macromol Sci B 53:1193–1204
6. Lee YR, Kim SC, Lee HI, Jeong HM, Raghu AV, Reddy KR, Kim BK (2011) Graphite oxides as effective fire retardants of epoxy resin. Macromol Res 19:66–71
7. Sehajpal SB, Sood VK (1989) Effect of metal fillers on some physical properties of acrylic resin. J Prosthet Dent 61(6):746–751
8. Zhang WD, Shen L, Phang IY, Liu T (2004) Carbon nanotubes reinforced nylon-6 composite prepared by simple melt-compounding. Macromolecules 37:256–259
9. Chen GX, Kim HS, Park BH, Yoon JS (2006) Multi-walled carbon nanotubes reinforced nylon 6 composites. Polymer 47:4760–4767
10. Coleman JN, Cadek M, Blake R, Nicolosi V, Ryan KP, Belton C, Fonseca A, Nagy JB, Gunko YK, Blau WJ (2004) High performance nanotube-reinforced plastics: understanding the mechanism of strength increase. Adv Funct Mater 14(8):791–798
11. Martin R, Mari D, Schaller R (2009) Influence of the carbon content on dislocation relaxation in martensitic steels. Mater Sci Eng, A 521–522:117–120
12. Tang WZ, Santare MH, Advani SG (2003) Melt processing and mechanical property characterization of multi-walled carbon nanotube/high density polyethylene (MWNT/HDPE) composite films. Carbon 41(14):2779–2785

13. Xiong JW, Zheng Z, Qin XM, Li M, Li HQ, Wang XL (2006) The thermal and mechanical properties of a poly-urethane/multi-walled carbon nanotube composite. Carbon 44(13):2701–2707
14. Saecd K, Park SY, Haider S, Baek JB (2009) In situ polymerization of multi-walled carbon nanotube/nylon-6 nanocomposites and their electrospun nanofibers. Nanoscale Res Lett 4:39–46
15. Prasad KE, Das B, Maitra U, Ramamurty U, Rao CNR (2009) Extra-ordinary synergy in the mechanical properties of polymer matrix composites reinforced with two nano-carbons of different dimensionalities. Proc Natl Acad Sci USA 106(32):13186–13189
16. Reddy KR, Lee KP, Gopalan AI, Showkat AM (2007) Synthesis and properties of magnetite/poly (aniline-co-8-amino-2-naphthalenesulfonic acid) (SPAN) nanocomposites. Polym Adv Technol 18:38–43
17. Reddy KR, Sin BC, Ryu KS, Kim JC, Chung HI, Lee YG (2009) Conducting polymer functionalized multi-walled carbon nanotubes with noble metal nanoparticles: synthesis, morphological characteristics and electrical properties. Synth Met 159:595–603
18. Dakshayini BS, Reddy KR, Mishra A, Shetti NP, Malode SJ, Basu S, Naveen S, Raghu AV (2019) Role of conducting polymer and metal oxide-based hybrids for applications in ampereometric sensors and biosensors. Microchem J 147:7–24
19. Reddy KR, Lee KP, Kee YI, Gopalan AI (2008) Facile synthesis of conducting polymer–metal hybrid nanocomposite by in situ chemical oxidative polymerization with negatively charged metal nanoparticles. Mater Lett 62:1815–1818
20. Khan MU, Reddy KR, Snguanwongchai T, Haque E, Gomes VG (2016) Polymer brush synthesis on surface modified carbon nanotubes via in situ emulsion polymerization. Colloid Polym Sci 294:1599–1610
21. McKeen LW (2010) Fatigue and tribological properties of plastics and elastomers, 2nd edn. Elsevier Inc., Amsterdam
22. Ahmad N, Gopinath P, Dutta R (2019) 3D printing technology in nanomedicine. Elsevier Inc., Amsterdam
23. Sood AK, Ohdar RK, Mahapatra SS (2010) Parametric appraisal of mechanical property of fused deposition modelling processed parts. Mater Des 31(1):287–295
24. Guvendiren M, Molde J, Soares RMD, Kohn J (2016) Designing biomaterials for 3D printing. ACS Biomater Sci Eng 2(10):1679–1693
25. Choi SH, Kim DH, Raghu AV, Reddy KR, Lee HI, Yoon KS, Jeong HM, Kim BK (2012) Properties of graphene/waterborne polyurethane nanocomposites cast from colloidal dispersion mixtures. J Macromol Sci B 51:197–207
26. Moon YK, Lee J, Lee JK, Kim TK, Kim SH (2009) Synthesis of length-controlled aerosol carbon nanotubes and their dispersion stability in aqueous solution. Langmuir 25:1739–1743
27. Kim WD, Huh JY, Ahn JY, Lee JB, Lee D, Hong SW, Kim SH (2012) Three-dimensional heterostructure of metallic nanoparticles and carbon nanotubes as potential nanofiller. Nanoscale Res Lett 7:202
28. American Society for Testing and Materials (1999) Annual book of ASTM standards: standard test methods for tensile properties of thin plastic sheeting. ASTM, Philadelphia
29. Oliver WC, Pharr GM (1992) An improved technique for determining hardness and elastic modulus using load and displacement sensing indentation experiments. J Mater Res 7(6):1564–1583
30. Lucas BN, Oliver WC (1999) Indentation power-law creep of high-purity indium. Metall Mater Trans A 30:601–610
31. Kulkarni MB, Bamboble VA, Mahanwar PA (2014) Effect of particle size of fly ash cenospheres on the properties of acrylonitrile butadiene styrene-filled composites. J Thermoplast Compos Mater 27(2):251–267
32. Koutavarapu R, Reddy CV, Babu B, Reddy KR, Cho M, Shim J (2020) Carbon cloth/transition metals-based hybrids with controllable architectures for electrocatalytic hydrogen evolution—a review. Int J Hydrogen Energy 45(3):7716–7740
33. Haque E, Kim J, Malgras V, Reddy KR, Ward AC, You J, Bando Y, Hossain MSA, Yamauchi Y (2018) Recent advances in graphene quantum dots: synthesis, properties, and applications. Small Methods 2:Article 1800050
34. Reddy KR, Sin BC, Yoo CH, Park W, Ryu KS, Lee JS, Sohn D, Lee Y (2008) A new one-step synthesis method for coating multi-walled carbon nanotubes with cuprous oxide nanoparticles. Scripta Mater 58(11):1010–1013
35. Torrado Perez AR, Roberson DA, Wicker RB (2014) Fracture surface analysis of 3D-printed tensile specimens of a novel ABS-based materials. J Fail Anal Prev 14(3):343–353

36. Reddy KR, Sin BC, Ryu KS, Noh J, Lee Y (2009) *In situ* self-organization of carbon black–polyaniline composites from nanospheres to nanorods: synthesis, morphology, structure and electrical conductivity. Synth Met 159:1934–1939
37. Jogi BF, Sawant M, Kulkarni M, Brahmankar PK (2012) Dispersion and performance properties of carbon nanotubes(CNTs) based polymer composites: a review. JEAS 2(4):69–78
38. Reddy NR, Bhargav U, Kumari MM, Cheralathan KK, Shankar MV, Reddy KR, Saleh TA, Aminabhavi TM (2020) Highly efficient solar light-driven photocatalytic hydrogen production over Cu/FCNTs-titania quantum dots-based heterostructures. J Environ Manag 254:Article 109747
39. Vairis A, Petousis M, Vidakis N, Savvakis K (2016) On the strain rate sensitivity of Abs and Abs plus fused deposition modeling parts. J Mater Eng Perform 25(9):3558–3565
40. Reddy RK, Reddy CHV, Nadagouda MN, Shetti NP, Jaesool S, Aminabhavi TM (2019) Polymeric graphitic carbon nitride (g-C_3N_4)-based semiconducting nanostructured materials: synthesis methods, properties and photocatalytic applications. J Environ Manag 238:25–40
41. Capaldi FM, Boyce MC, Rutledge GC (2002) Enhanced mobility accompanies the active deformation of a glassy amorphous polymer. Phys Rev Lett 89:117505
42. Haque E, Yamauchi Y, Malgras V, Reddy KR, Yi JW, Hossain MSA, Kim J (2018) Nanoarchitectured graphene-organic frameworks (GOFs): synthetic strategies, properties, and applications. Chem Asian J 13:3561–3574
43. Amit M, Shetti NP, Basu S, Reddy KR, Aminabhavi TM (2019) Carbon cloth-based hybrid materials as flexible electrochemical supercapacitors. ChemElectroChem 6:5771–5786
44. Kiener D, Minor AM, Anderoglu O, Wang YQ, Maloy SA, Hosemann P (2012) Application of small-scale testing for investigation of ion-beam-irradiated materials. J Mater Res 27(21):2724–2736
45. Wang H, Zhu L, Xu B (2018) Residual stresses and nanoindentation testing of films and coatings. Springer Nature, Singapore